Online ISSN 1848-3380, Print ISSN 0005-1144
ATKAFF 57(3), 578–588(2016)

M. Kutija, D. Sumina, I. Čolović

PLL-based Rotor Flux Estimation Method for Sensorless Vector Controlled Squirrel-Cage Induction Generators

DOI 10.7305/automatika.2016.11.1940
UDK 681.516.77.015.42:621.313.332.045.56.013-854

Original scientific paper

This paper presents a new rotor flux estimation method for sensorless vector controlled squirrel-cage induction generators used in wind power applications. The proposed method is based on a phase-locked loop (PLL) and the orthogonality between the rotor flux space vector and its back electromotive force (EMF) space vector. Rotor flux is estimated using stator voltage equations without integrating the back EMF components in the stationary reference frame and the well-known difficulties with the implementation of pure integrators are thus avoided. Moreover, the proposed method ensures successful magnetization of a speed-sensorless squirrel-cage induction generator at non-zero speeds which makes it suitable for wind power applications. Experimental results on a 560 kW squirrel-cage induction generator are presented to confirm the effectiveness and the feasibility of the proposed method.

Key words: Induction generator, Flux estimation, Phase locked loop (PLL), Sensorless control, Vector control, Wind power generation

Metoda za estimaciju magnetskog toka rotora kaveznih asinkronih generatora bez mjernog člana brzine vrtnje temeljena na fazno spregnutoj petlji. U radu je predstavljena nova metoda za estimaciju magnetskog toka rotora vektorski upravljanih kaveznih asinkronih vjetrogeneratora. Predložena metoda se temelji na fazno spregnutoj petlji i ortogonalnosti između prostornog vektora magnetskog toka rotora i njemu pripadajućeg prostornog vektora induciranog napona. Magnetski tok rotora se estimira korištenjem naponskih jednadžbi statora u koordinatnom sustavu statora bez integracije komponenti induciranog napona čime su izbjegnuti dobro poznati problemi implementacije integratora. Osim toga, predložena metoda omogućava uspješno magnetiziranje pri vrtnji kaveznog asinkronog generatora bez mjernog člana brzine vrtnje pa je pogodna za primjenu na vjetrogeneratorima. U radu su prikazani eksperimentalni rezultati za kavezni asinkroni generator snage 560 kW koji potvrđuju izvedivost i učinkovitost predložene metode.

Ključne riječi: asinkroni generator, estimacija magnetskog toka, fazno spregnuta petlja, bezsenzorsko upravljanje, vektorsko upravljanje, proizvodnja električne energije iz vjetra

1 INTRODUCTION

Squirrel cage induction generator (SCIG) with a full-scale power converter has been receiving increasing attention over the past few years for variable speed wind energy conversion systems (WECSs) [1–3]. The well-known advantages of a SCIG such as its robustness, reliability, low price, low maintenance requirements and costs coupled with permanent price reductions of power electronic devices, made the SCIG with a full-scale power converter an attractive choice for wind power generation [4]. The SCIG used in a variable speed WECS is usually connected to the grid through a back-to-back voltage source converter (VSC) as shown in Fig. 1. Torque and flux control of the SCIG is achieved by using the generator-side inverter and active and reactive power control of a WECS is achieved by using the grid-side inverter.

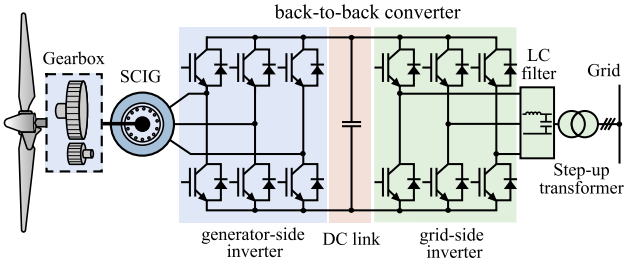

Fig. 1. Structure of the variable-speed wind power generation system with the SCIG

For the torque and flux control of the SCIG, rotor field oriented vector control (RFOC) is used. The RFOC is based on the rotor flux orientation which allows torque

and flux to be decoupled and controlled independently. Since all machine states and outputs needed for the flux and torque control feedback are calculated by using the estimated flux vector, the performance of vector controlled induction machines depends greatly on the accuracy of the estimated flux [5–7]. Furthermore, the risk of degraded performance and instability due to the incorrect flux estimation increases tremendously if sensorless control is used [8]. What complicates the sensorless control is the difficulty of accurately estimating the rotor flux without speed measurement. An additional issue for sensorless vector controlled SCIGs used in wind power applications is the magnetization process at non-zero speeds which is difficult to achieve when speed information is not available [9].

Generally, there are two basic approaches to flux estimation in sensorless vector controlled induction machines [5,10]. Two competing methodologies are model based estimation methods which rely on the fundamental machine model and signal injection estimation methods, which exploit the anisotropic properties of the machine excited with additional high-frequency test signals. The signal injection estimation methods are beyond the scope of this paper as they depend on particular machine design. The model based estimation methods can be classified as open loop estimators, Model Reference Adaptive System (MRAS) and adaptive flux observers. The open loop estimators, such as the voltage model flux estimator and the current model flux estimator, estimate the rotor flux without feedback correction [11]. The MRAS observers estimate the rotor flux and speed by comparing the reference model and the adjustable model [12]. The adjusting signal driving the adaptation mechanism may be based on rotor flux [13–15], back EMF [16, 17], or reactive power [18–20]. The adaptive flux observers can be classified as deterministic observers, such as the Luenberger observer [21, 22], sliding mode observers [23–25], and stochastic observers, such as the extended Kalman filter [26–28]. Furthermore, neural network based observers are also used for flux estimation [29, 30].

Although the aforementioned methods are developed for induction motors, they can be used for induction generators as well. However, the requirements on the sensorless flux estimation methods for induction motors and SCIGs used in wind power applications are different. The main issue for speed sensorless induction motors is flux estimation at low speeds and zero speed. On the other hand, the SCIGs used in wind power applications do not operate at low speeds but require successful magnetization at non-zero speeds. In order to achieve successful magnetization of the SCIGs at non-zero speeds, the existing sensorless model based flux estimation methods have to be upgraded with a synchronization algorithm [9].

For that reason, this paper proposes a new rotor flux estimation method which can magnetize sensorless vector controlled SCIG at non-zero speeds and is, therefore, suitable for use in wind power applications. The proposed method is rather simple to implement, uses minimum processor time and memory and can be used with wind generation systems of high nominal power. The method is based on a PLL and the orthogonality between the rotor flux space vector and its back EMF vector. The idea of using PLL comes from control of grid-connected power converters where PLL is used for synchronization with the utility voltages [31–33]. Although the proposed method is derived from voltage model flux estimator, rotor flux is estimated without integrating the back EMF vector components in stationary reference frame. As a result, the implementation issues associated with voltage model based estimators are avoided and the accuracy of the estimated flux angle does not depend on the implementation of the integrator. The proposed method is implemented in a digital control system and validated through the experimental tests. Experimental tests were conducted on a 560 kW SCIG.

This paper is organized as follows. The voltage model flux estimator and implementation issues are introduced in Section 2. The new rotor flux estimation method is designed and analysed in Section 3. Finally, the experimental results are presented in Section 4.

2 VOLTAGE MODEL FLUX ESTIMATOR

Voltage model flux estimator (VI), also referred to as voltage model (VM), is inherently a sensorless open loop estimator which obtains the rotor flux by integrating its back EMF in the stationary reference frame. It is based on the stator voltage equation and flux linkage equations written in the stationary reference frame as follows:

$$\boldsymbol{u_s} = R_s \boldsymbol{i_s} + \frac{d\boldsymbol{\psi_s}}{dt} \tag{1}$$

$$\boldsymbol{\psi_s} = L_s \boldsymbol{i_s} + L_m \boldsymbol{i_r} \tag{2}$$

$$\boldsymbol{\psi_r} = L_m \boldsymbol{i_s} + L_r \boldsymbol{i_r} \tag{3}$$

where $\boldsymbol{\psi_s}$, $\boldsymbol{\psi_r}$, $\boldsymbol{u_s}$, $\boldsymbol{i_s}$ and $\boldsymbol{i_r}$ are space vectors of the stator and rotor flux, the stator voltage, the stator current and the rotor current, respectively. R_s, L_s, L_m and L_r are the stator resistance, the stator inductance, the magnetizing inductance and the rotor inductance, respectively. By substituting (2) and (3) in (1), the rotor flux is obtained as follows:

$$\boldsymbol{\psi_r} = \frac{L_r}{L_m} \left[\int (\boldsymbol{u_s} - R_s \boldsymbol{i_s})\, dt - \sigma \cdot L_s \boldsymbol{i_s} \right] \tag{4}$$

The total leakage factor σ is expressed as follows:

$$\sigma = 1 - \frac{L_m^2}{L_s L_r} \tag{5}$$

The major weakness of the voltage model flux estimator is the implementation of a pure integrator which suffers from DC drift and initial value problems [34, 35]. In order to overcome these problems, numerous methods with different modifications of the voltage model flux estimator have been proposed in literature. Most of the proposed voltage model based methods replace the pure integrator by the first-order low pass filter (LPF) with either a fixed [34,36,37], or a variable cut-off frequency [6,35,38]. However, the use of LPF introduces the phase and magnitude errors in the estimated flux and requires a compensation algorithm to compensate these errors. Furthermore, the flux estimation methods with pure integration and an error compensation algorithm have also been reported [39, 40]. Hence, all of the proposed voltage model based methods require an error compensation algorithm in order to compensate the integration errors.

3 PROPOSED ESTIMATION METHOD

The core of a RFOC system is the flux estimator and the key quantity is the rotor flux angle. An accurate rotor flux angle provides decoupling of torque-generating current and flux-generating current and enables high performance control of the SCIG. On the other hand, an incorrect flux angle leads to undesirable cross coupling of flux and torque control loops, deterioration of the overall drive performance and instability. For practical use, less complex flux estimators are preferred [11]. The simplest way of obtaining the rotor flux is by integrating its back EMF but this approach has implementation problems discussed in the previous section. The phase angle between the rotor flux vector and the back EMF vector is 90 degrees. When an integration error occurs, the phase angle between the estimated flux vector and the back EMF vector is no longer 90 degrees, which deteriorates the RFOC performance [34]. An ideal voltage model based flux estimation method should ensure the orthogonality of the estimated rotor flux and the back EMF in the whole operating range of the induction machine, which would result from an analytical integration of (4). Such a method is not available at present.

However, the integration of a space vector can be achieved by simple rotation of the vector by 90 degrees in the negative direction and scaling its magnitude with respect to its angular frequency. The proposed rotor flux estimation method uses this principle for the integration of the back EMF and thus avoids the implementation of a pure integrator or an LPF. As a result, the orthogonality between the back EMF space vector and the rotor flux vector is preserved in the whole operating range of the induction machine, an error compensation algorithm is not needed and an extremely simple flux estimation method is obtained. Moreover, unlike the other sensorless model based flux estimation methods, the proposed method can successfully magnetize the SCIGs at non-zero speeds. However, the estimation of the rotor flux is not possible at zero speed and thus, this method cannot be used for induction motors.

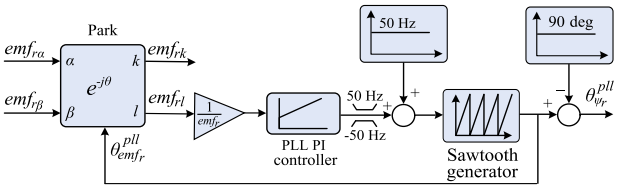

Fig. 2. Block diagram of the proposed method

3.1 Flux estimation

The proposed method is composed of the back EMF estimator and a PLL as shown in Fig. 2. The back EMF vector is obtained in the stationary reference frame from the induction machine model by using stator voltages and stator currents as follows:

$$emf_{r\alpha} = \frac{L_r}{L_m}\left[u_{s\alpha} - R_s i_{s\alpha} - \sigma L_s \frac{di_{s\alpha}}{dt}\right] \tag{6}$$

$$emf_{r\beta} = \frac{L_r}{L_m}\left[u_{s\beta} - R_s i_{s\beta} - \sigma L_s \frac{di_{s\beta}}{dt}\right] \tag{7}$$

where $\boldsymbol{emf_r}$ represents the back EMF vector and α and β denote space vector components in the stationary reference frame. In practice, if the back EMF angle is directly calculated from $emf_{r\alpha}$ and $emf_{r\beta}$ components using *arctan* function, a deformed angle may be obtained and unstable operation of the flux estimator may occur. To achieve stable operation of the flux estimator and less noise sensitive estimation of the back EMF angle, the PLL is used.

Since the d-axis of the synchronous dq reference frame is oriented along the rotor flux space vector, only the q component of the back EMF vector exists in a steady state. The estimated dq axes used in the digital control system are denoted by superscript dsp and the actual dq reference frame axes are not denoted by superscript. By regulating the d^{dsp} component of the back EMF vector to zero, the PLL feedback loop detects the angular position of the back EMF vector. Therefore, the output of the feedback loop is the back EMF angle $\theta^{pll}_{emf_r}$ and the rotor flux angle $\theta^{pll}_{\psi_r}$ is

easily obtained by rotating the estimated back EMF vector by 90 degrees in the negative direction, i.e. by subtracting 90 degrees from the estimated back EMF angle $\theta^{pll}_{emf_r}$.

To estimate the back EMF angle the PLL uses the synchronous reference frame, in this paper denoted as kl frame, whose real k-axis is aligned with the back EMF vector. The back EMF vector is translated from the $\alpha\beta$ stationary reference frame to the kl synchronous reference frame by using Park's transformation and the estimated back EMF angle as follows:

$$\begin{bmatrix} emf_{rk} \\ emf_{rl} \end{bmatrix} = \begin{bmatrix} \cos\theta^{pll}_{emf_r} & \sin\theta^{pll}_{emf_r} \\ -\sin\theta^{pll}_{emf_r} & \cos\theta^{pll}_{emf_r} \end{bmatrix} \begin{bmatrix} emf_{r\alpha} \\ emf_{r\beta} \end{bmatrix} \quad (8)$$

The synchronous kl reference frame rotates at the same speed as the $d^{dsp}q^{dsp}$ frame, but its real k-axis is shifted 90 degrees in the positive direction with respect to the d^{dsp}-axis of the $d^{dsp}q^{dsp}$ reference frame, as shown in Fig. 3. Obviously, the expressions $emf_{rk} = emf_{rq}$ and $emf_{rl} = -emf_{rd}$ apply. The PLL PI controller synchronizes the kl reference frame with the back EMF vector by keeping the emf_{rl}, i.e. emf_{rd} component equal to zero.

Using (8), the back EMF vector components in the natural abc reference frame and the Clarke transformation, the emf_{rk} and emf_{rl} components are given by:

$$\begin{bmatrix} emf_{rk} \\ emf_{rl} \end{bmatrix} = emf_r \begin{bmatrix} \cos\left(\theta_{emf_r} - \theta^{pll}_{emf_r}\right) \\ \sin\left(\theta_{emf_r} - \theta^{pll}_{emf_r}\right) \end{bmatrix} \quad (9)$$

where emf_r represents the back EMF vector magnitude and θ_{emf_r} represents the actual back EMF angle. If the error between the estimated $d^{dsp}q^{dsp}$ and the actual dq reference frame $\Delta\theta = \theta_{emf_r} - \theta^{pll}_{emf_r}$ is set to zero, the d-axis and the d^{dsp}-axis are aligned and the back EMF vector is positioned in the q-axis. When an error between the estimated and the actual back EMF angle occurs, the emf_{rd} component of the back EMF vector is presented as shown in Fig. 3. The PLL PI controller aligns the estimated $d^{dsp}q^{dsp}$ reference frame with the actual dq reference frame by regulating the emf_{rd} component of the back EMF vector to zero.

The selection of the PLL PI controller parameters is based on the small-signal analysis [31], which assumes that the phase difference $\Delta\theta$ is very small and the PLL can be linearized as:

$$\sin\left(\theta_{emf_r} - \theta^{pll}_{emf_r}\right) \approx \theta_{emf_r} - \theta^{pll}_{emf_r} \quad (10)$$

According to (9), the back EMF vector magnitude emf_r, which is speed dependable, appears as a gain term in the linearized model of the PLL system and causes a loss of gain of the PLL loop when operating below the rated frequency. In order to eliminate this effect, the emf_{rl} component is normalized with the back EMF vector magnitude emf_r as shown in Fig. 2. For the selection of the PLL control parameters, symmetrical optimum is used. It should be noted that the design of the PLL is a trade-off between fast tracking and good filtering characteristics. If the PLL control parameters are adjusted properly, the accuracy of the estimated rotor flux depends only on the accuracy of the estimated back EMF space vector.

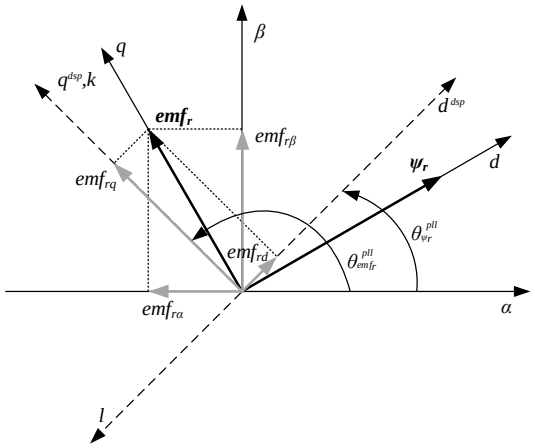

Fig. 3. Relation between the rotor flux vector and the back EMF vector

The rotor flux magnitude is also estimated from the back EMF vector. In the steady state, the back EMF vector is aligned with the k-axis and the emf_{rk} component represents the back EMF vector magnitude. Therefore, the rotor flux magnitude can be estimated as follows:

$$\psi_r = \frac{emf_{rk}}{\omega_s} \quad (11)$$

where ψ_r represents the rotor flux magnitude estimated from the back EMF and ω_s represents the synchronous speed. When an error between the estimated and the actual back EMF angle occurs, the back EMF vector is not aligned with the k-axis and the rotor flux magnitude estimated according to (11) differs from the actual rotor flux magnitude. However, this error is negligible for small angles of misalignment.

3.2 Magnetization

The method proposed in this paper is also able to magnetize the speed-sensorless rotating SCIG in the whole operating range and it can be applied to standard induction

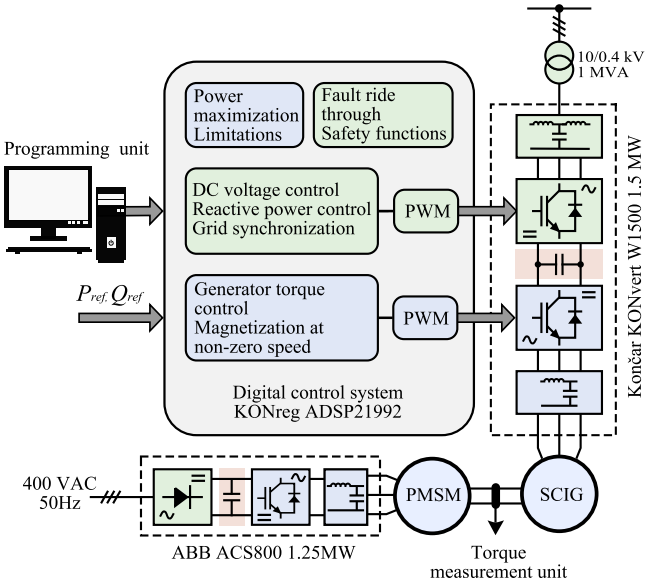

Fig. 4. Experimental setup

machines. The main issue of the magnetization process at non-zero speeds is to determine the generator supply frequency which should be applied to a rotating SCIG in order to magnetize it. This is achieved by adding a constant value which corresponds to the angle increment of the rated frequency to the PLL PI controller output as shown in Fig. 2. When the back-to-back converter is turned on, the PLL PI controller changes the inverter output frequency from the rated frequency to the required synchronous frequency, which is equal to the sum of the rotor frequency and slip frequency. At the same time, the torque-generating current is regulated to zero. When the required synchronous frequency is detected, magnetization of the SCIG starts. When the magnetization process is started, the proposed method estimates the rotor flux angle. Additional details regarding the magnetization process can be found in [9].

4 EXPERIMENTAL VERIFICATION

The validity of the proposed method has been tested experimentally and confirmed as follows. The tests were performed on the experimental setup presented in Fig. 4. The test rig is made up of a SCIG connected to the grid via a back-to-back converter KONČAR KONvert W1500 and mechanically coupled with a permanent magnet synchronous motor (PMSM) via a torque measurement unit. The PMSM, emulating a wind turbine, is fed by the frequency converter ABB ACS800. The test rig is shown in Fig. 5. General data are as follows.

SCIG: Končar 8AZJ 405-04, 560 kW, 400 V, 967 A, 50 Hz, 1490 r/min, cosϕ = 0.87, delta connection. The

Fig. 5. Laboratory test rig

machine was initially constructed to work as a motor and in this investigation it was used as a generator. The base values were set as follows: 1367 A, 326 V, 314 rad/s, 0.239 Ω. The parameters were as follows: L_m = 3.33 p.u., $L_r = L_s$ = 3.442 p.u., R_s = 0.0053 p.u., R_r = 0.0083 p.u.. The SCIG speed was measured via an incremental encoder, but it was not used in the sensorless vector control.

Back-to-back converter: KONČAR KONvert W1500, 1.5 MW, 690 V, 1480 A, using a 2 kHz switching frequency and 650 V DC-link voltage. The digital control system is based on an Analog Devices ADSP-21992 16-bit fixed-point digital signal processor.

SMPM: Tema Pula LPMR-450, 375 kW, 400 V, 596 A, 75 Hz, 1500 r/min. A resolver was used for speed and position measurement.

Frequency converter: ABB ACS800, 1.25 MW, 500 V, 1596 A, and 580 V DC-link voltage.

The proposed algorithm is implemented in a digital control system and tested under various conditions. The simplified overall structure of the control system is depicted in Fig. 6. For the torque and flux control of the SCIG, the RFOC was used. The torque-generating current reference was calculated from the torque reference and the flux reference was set to its nominal value. The flux magnitude calculated according to (11) was used in the control structure and the flux angle was estimated by the proposed algorithm. The stator voltage was estimated by using DC bus voltage and PWM pulses, with deadtime and conducting voltage compensated. The system is speed-sensorless since speed signal is not used for the flux estimation. Experimental results were recorded by using the digital control system and then transferred to a PC via an optical link.

The performed experimental tests can be classified into three groups: magnetization tests, steady state perfor-

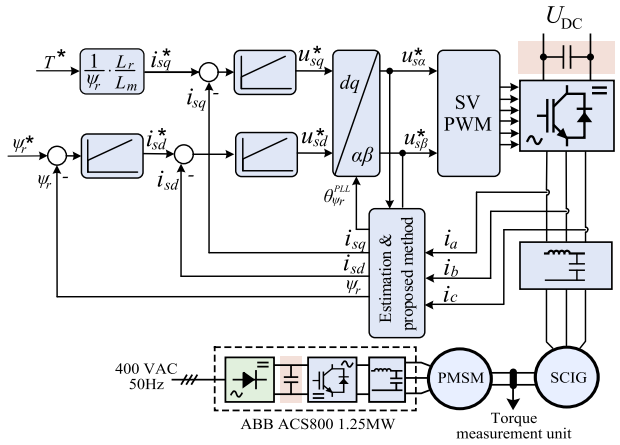

Fig. 6. Block diagram of the control structure

mance tests and dynamic performance tests. The experimental results with a detailed discussion are given as follows.

4.1 Magnetization

The experimental results of the magnetization tests are given at the rotor speed of 500 rpm which represents a cut-in speed for the SCIG used in wind power applications. At the beginning, the speed of the PMSM is set to 500 rpm, the back-to-back converter is turned off and the SCIG is, clearly, rotating at the same speed as the PMSM. At 0 s the magnetization process begins by starting the back-to-back converter. During the magnetization process the torque-generating current is kept at zero value. Corresponding results are shown in Fig. 7.

It can be observed that during this test the SCIG was successfully magnetized. The PLL PI controller changed the output frequency of the back-to-back converter until the synchronous frequency corresponding to the actual speed was reached. At that moment flux started to build. The time needed for the magnetization process to be completed depends on the tuning of the PLL PI controller, shaft speed, actual rotor time constant and the value of the field-generating current.

4.2 Steady state performance

The performance of the proposed method in the steady state is tested in the whole operating range of the SCIG under various loads. In this paper, the experimental results will be given for the no load steady state operation of the SCIG at 500 rpm. The experimental results are presented in Fig. 8.

Figure 8 shows that there are no distortions in the estimated flux angle. Furthermore, the phase difference between the back-EMF components and the related estimated

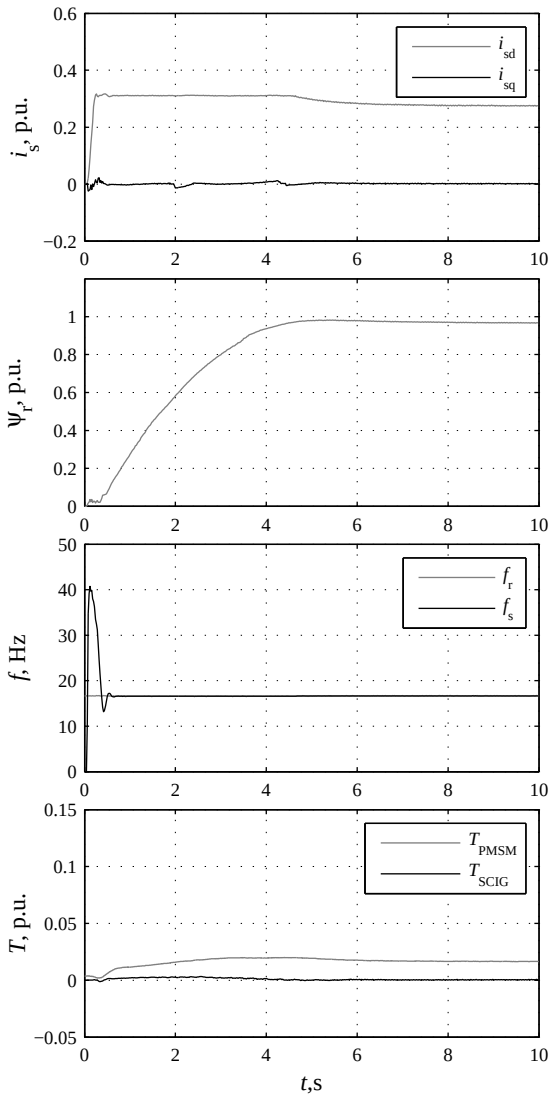

Fig. 7. Experimental results showing magnetization process of SCIG at rotor speed of 500 rpm. The first subplot shows the field-generating current (i_{sd}) and the torque-generating current (i_{sq}), the second subplot shows the flux magnitude estimated by the proposed method (ψ_r), the third subplot shows the rotor speed frequency (f_r) and the synchronous frequency (f_s), and the last subplot shows the measured torque supplied by the prime mover (T_{PMSM}) and the estimated electromagnetic torque of the SCIG (T_{SCIG}).

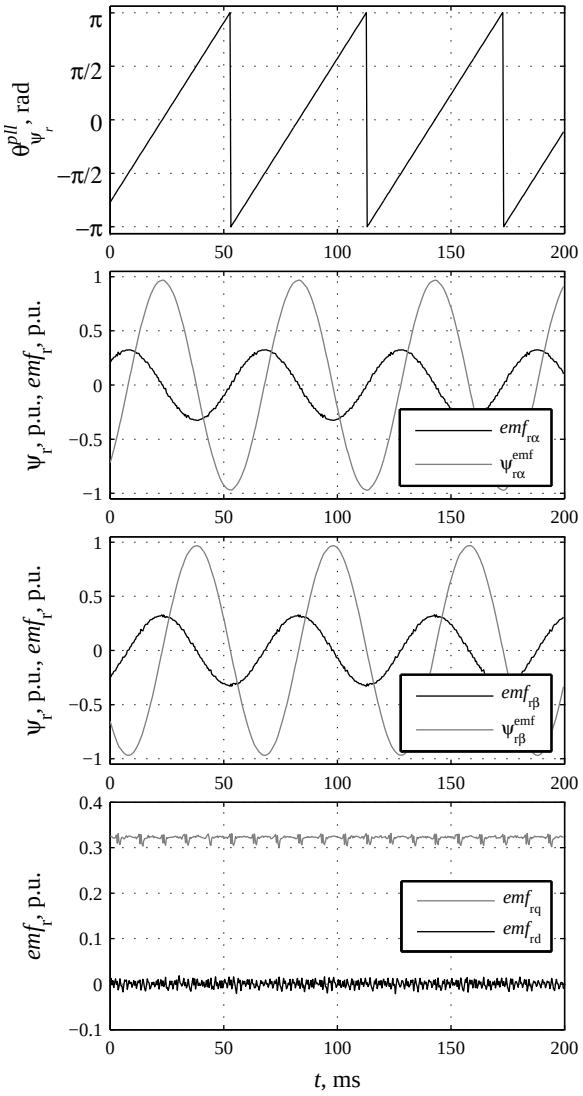

Fig. 8. Experimental results showing no load steady state operation of SCIG at rotor speed of 500 rpm. The first subplot shows the flux angle estimated by the proposed method ($\theta_{\psi r}^{pll}$), the second and the third subplot show the α, β components of the rotor back-EMF (emf_r) and the α, β components of the rotor flux estimated by the proposed method (ψ_r), and the last subplot shows the back EMF vector components in the synchronous dq reference frame.

flux components is 90 degrees and there is no DC offset in the estimated back-EMF and flux components. The emf_{rq} component is constant and the emf_{rd} component is kept at zero value.

4.3 Dynamic performance

The dynamic performance of the proposed flux estimator is also verified by experimental tests. Two different experiments were carried out: a change in the PMSM speed reference from 500 rpm to 800 rpm and a change in the SCIG torque reference from 0 p.u. to 0.3 p.u.

Fig. 9 shows experimental results for the PMSM speed reference change from 500 rpm to 800 rpm. The SMPM speed reference ramp was set to 10 s from zero to the rated speed. As can be seen from Fig. 9, the estimated synchronous frequency follows the change in the rotor speed frequency. The flux magnitude and the stator current components remain unchanged.

The dynamic performance of the proposed method is also investigated by conducting experimental tests of the SCIG torque reference changes. The tests included applying the ramped torque reference and observing the estimated synchronous frequency. The SCIG torque reference ramp was set to 14 s from zero to the rated torque. The experimental results are shown in Fig. 10. The system was in the steady state at the rotor speed of 500 rpm and the torque reference of 1068 Nm (30% of the rated load) at t=0.5 s was applied. Fig. 10 shows that the estimated synchronous frequency follows the change of the rotor speed frequency. The emf_{rq} component changes slightly and the flux magnitude remains the same.

5 CONCLUSION

This paper proposes a new speed-sensorless flux estimation method which is usable with standard induction generators, able to magnetize induction generators at non-zero speeds, exhibits high dynamic performance and its digital implementation is computationally efficient. The proposed method estimates the rotor flux from its back-EMF by using a PLL and the orthogonality relation between the back EMF space vector and the flux space vector. As a result, the well-known integration problems are avoided and the accuracy of the estimated flux angle mainly depends on the quality of the estimated back-EMF vector. The PLL PI controller also provides speed-sensorless magnetization of a SCIG at non-zero speeds which makes the proposed method highly suitable for SCIGs used in wind power generation systems.

The method is implemented into a digital control system and its steady-state and dynamic performance are experimentally verified. The experimental results show excellent performance and confirm that the method is highly

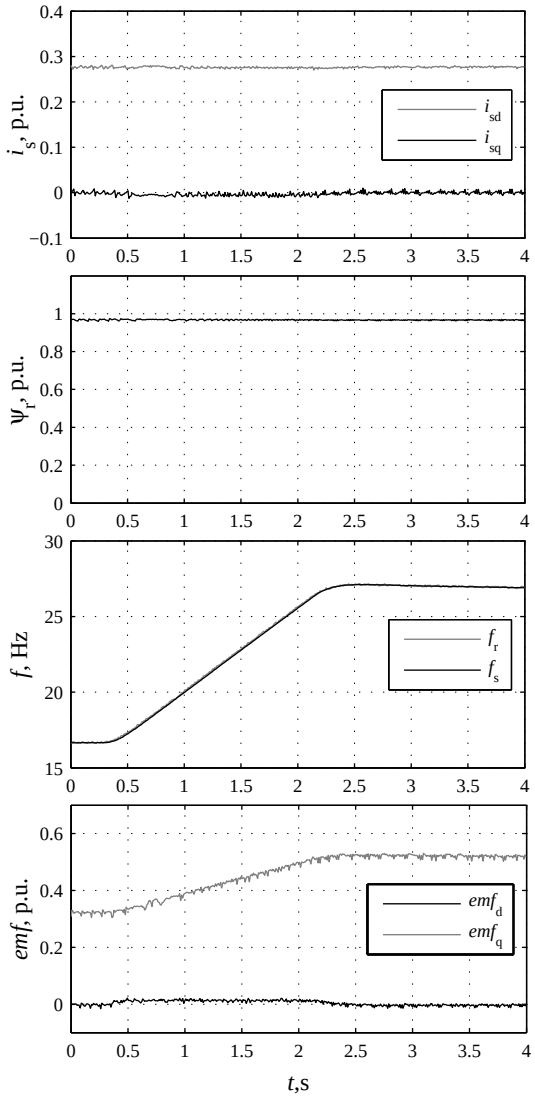

Fig. 9. Experimental results for speed change from 500 rpm to 800 rpm. The first subplot shows the field-generating current (i_{sd}) and the torque-generating current (i_{sq}), the second subplot shows the flux magnitude estimated by the proposed method (ψ_r), the third subplot shows the rotor speed frequency (f_r) and the synchronous frequency (f_s), and the last subplot shows the back EMF vector components in the synchronous dq reference frame.

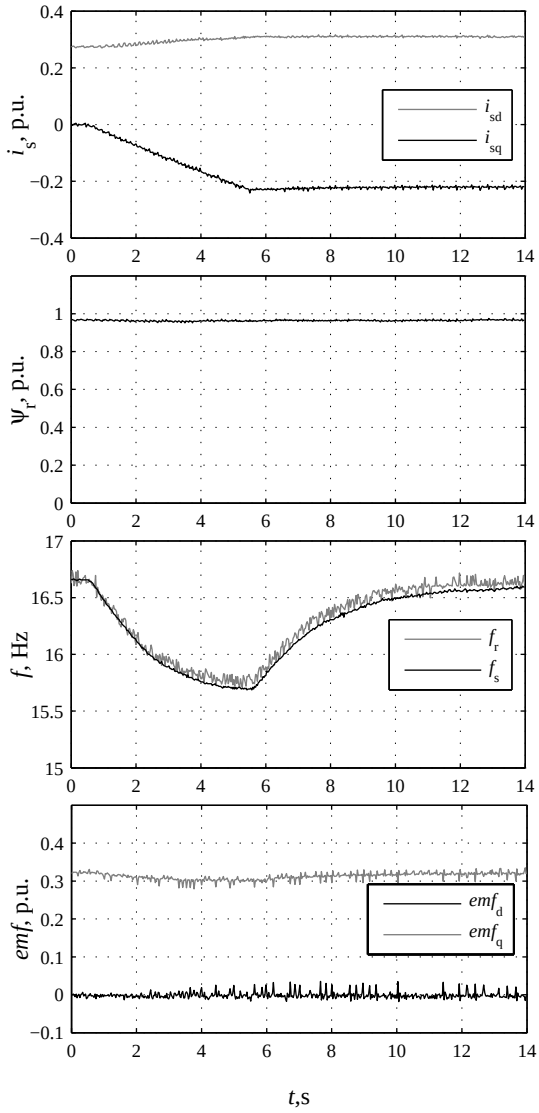

Fig. 10. Experimental results for ramped torque reference at 500 rpm. The first subplot shows the field-generating current (i_{sd}) and the torque-generating current (i_{sq}), the second subplot shows the flux magnitude estimated by the proposed method (ψ_r), the third subplot shows the rotor speed frequency (f_r) and the synchronous frequency (f_s), and the last subplot shows the back EMF vector components in the synchronous dq reference frame.

appropriate for wind power applications. However, the proposed flux estimation method cannot be used for induction motors because it is not able to estimate the rotor flux at zero speed.

ACKNOWLEDGMENT

This work was supported in part by the Končar - Electronics and Informatics Inc. through the Project "Development and Implementation of Vector Control Structures for Wind Turbine Induction Generator" 73474-2012.

REFERENCES

[1] V. Yaramasu, B. Wu, P. Sen, S. Kouro, and M. Narimani, "High-power wind energy conversion systems: State-of-the-art and emerging technologies," *Proceedings of the IEEE*, vol. 103, no. 5, pp. 740–788, 2015.

[2] F. Blaabjerg and K. Ma, "Future on power electronics for wind turbine systems," *Emerging and Selected Topics in Power Electronics, IEEE Journal of*, vol. 1, no. 3, pp. 139–152, 2013.

[3] H. Polinder, J. Ferreira, B. Jensen, A. Abrahamsen, K. Atallah, and R. McMahon, "Trends in wind turbine generator systems," *Emerging and Selected Topics in Power Electronics, IEEE Journal of*, vol. 1, no. 3, pp. 174–185, 2013.

[4] V. Agarwal, R. K. Aggarwal, P. Patidar, and C. Patki, "A novel scheme for rapid tracking of maximum power point in wind energy generation systems," *Energy Conversion, IEEE Transactions on*, vol. 25, no. 1, pp. 228–236, 2010.

[5] J. Holtz, "Sensorless control of induction machines - with or without signal injection?," *Industrial Electronics, IEEE Transactions on*, vol. 53, no. 1, pp. 7–30, 2006.

[6] M. Comanescu and L. Xu, "An improved flux observer based on pll frequency estimator for sensorless vector control of induction motors," *Industrial Electronics, IEEE Transactions on*, vol. 53, no. 1, pp. 50–56, 2006.

[7] D. P. Marcetic, I. R. Krcmar, M. A. Gecic, and P. R. Matic, "Discrete rotor flux and speed estimators for high-speed shaft-sensorless im drives," *Industrial Electronics, IEEE Transactions on*, vol. 61, no. 6, pp. 3099–3108, 2014.

[8] L. Harnefors and M. Hinkkanen, "Stabilization of sensorless induction motor drives: A survey," in *Electrical Machines Design Control and Diagnosis (WEMDCD), 2013 IEEE Workshop on*, pp. 183–192, IEEE, 2013.

[9] M. Kutija, D. Sumina, and I. Čolović, "Magnetization of speed sensorless squirrel-cage induction generator for wind power application using a phase-locked loop," *Electric power systems research*, vol. 122, pp. 119–129, 2015.

[10] D. P. Marcetic and S. N. Vukosavic, "Speed-sensorless ac drives with the rotor time constant parameter update," *Industrial Electronics, IEEE Transactions on*, vol. 54, no. 5, pp. 2618–2625, 2007.

[11] L. Harnefors and M. Hinkkanen, "Stabilization methods for sensorless induction motor drives—a survey," *Emerging and Selected Topics in Power Electronics, IEEE Journal of*, vol. 2, no. 2, pp. 132–142, 2014.

[12] R. Kumar, S. Das, P. Syam, and A. Chattopadhyay, "Review on model reference adaptive system for sensorless vector control of induction motor drives," *Electric Power Applications, IET*, vol. 9, no. 7, pp. 496–511, 2015.

[13] I. Benlaloui, S. Drid, L. Chrifi-Alaoui, and M. Ouriagli, "Implementation of a new mras speed sensorless vector control of induction machine," *Energy Conversion, IEEE Transactions on*, vol. 30, no. 2, pp. 588–595, 2015.

[14] R. Cardenas and R. Pena, "Sensorless vector control of induction machines for variable-speed wind energy applications," *Energy Conversion, IEEE Transactions on*, vol. 19, no. 1, pp. 196–205, 2004.

[15] V. Vasic, S. N. Vukosavic, and E. Levi, "A stator resistance estimation scheme for speed sensorless rotor flux oriented induction motor drives," *Energy Conversion, IEEE Transactions on*, vol. 18, no. 4, pp. 476–483, 2003.

[16] N. Bensiali, E. Etien, and N. Benalia, "Convergence analysis of back-emf mras observers used in sensorless control of induction motor drives," *Mathematics and Computers in Simulation*, vol. 115, pp. 12 – 23, 2015.

[17] M. Rashed and A. Stronach, "A stable back-emf mras-based sensorless low-speed induction motor drive insensitive to stator resistance variation," *IEE Proceedings-Electric Power Applications*, vol. 151, no. 6, pp. 685–693, 2004.

[18] A. Ravi Teja, V. Verma, and C. Chakraborty, "A new formulation of reactive-power-based model reference adaptive system for sensorless induction motor drive," *Industrial Electronics, IEEE Transactions on*, vol. 62, no. 11, 2015.

[19] V. Jevremovic, V. Vasic, D. Marcetic, and B. Jeftenic, "Speed-sensorless control of induction motor based on reactive power with rotor time constant identification," *Electric Power Applications, IET*, vol. 4, no. 6, pp. 462–473, 2010.

[20] S. Maiti and C. Chakraborty, "A new instantaneous reactive power based mras for sensorless induction motor drive," *Simulation Modelling Practice and Theory*, vol. 18, no. 9, pp. 1314–1326, 2010.

[21] S. Di Gennaro, J. Rivera Dominguez, and M. Meza, "Sensorless high order sliding mode control of induction motors with core loss," *Industrial Electronics, IEEE Transactions on*, vol. 61, no. 6, pp. 2678–2689, 2014.

[22] I. Vicente, A. Endemaõo, X. Garin, and M. Brown, "Comparative study of stabilising methods for adaptive speed sensorless full-order observers with stator resistance estimation," *Control Theory Applications, IET*, vol. 4, no. 6, pp. 993–1004, 2010.

[23] L. Zhao, J. Huang, H. Liu, B. Li, and W. Kong, "Second-order sliding-mode observer with online parameter identification for sensorless induction motor drives," *Industrial Electronics, IEEE Transactions on*, vol. 61, no. 10, pp. 5280–5289, 2014.

[24] J. Rivera Dominguez, "Discrete-time modeling and control of induction motors by means of variational integrators and sliding modes—part ii: Control design," *Industrial Electronics, IEEE Transactions on*, vol. 62, no. 10, pp. 6183–6193, 2015.

[25] M. Comanescu, "Design and implementation of a highly robust sensorless sliding mode observer for the flux magnitude of the induction motor," *IEEE Transactions on Energy Conversion*, vol. 31, no. 2, pp. 649–657, 2016.

[26] M. Barut, S. Bogosyan, and M. Gokasan, "Speed-sensorless estimation for induction motors using extended kalman filters," *Industrial Electronics, IEEE Transactions on*, vol. 54, no. 1, pp. 272–280, 2007.

[27] F. Alonge, T. Cangemi, F. D'Ippolito, A. Fagiolini, and A. Sferlazza, "Convergence analysis of extended kalman filter for sensorless control of induction motor," *Industrial Electronics, IEEE Transactions on*, vol. 62, no. 4, pp. 2341–2352, 2015.

[28] M. Habibullah and D.-C. Lu, "A speed-sensorless fs-ptc of induction motors using extended kalman filters," *Industrial Electronics, IEEE Transactions on*, vol. 62, no. 11, pp. 6765–6778, 2015.

[29] S. M. Gadoue, D. Giaouris, and J. W. Finch, "Sensorless control of induction motor drives at very low and zero speeds using neural network flux observers," *Industrial Electronics, IEEE Transactions on*, vol. 56, no. 8, pp. 3029–3039, 2009.

[30] S. Gadoue, D. Giaouris, and J. Finch, "Stator current model reference adaptive systems speed estimator for regenerating-mode low-speed operation of sensorless induction motor drives," *Electric Power Applications, IET*, vol. 7, no. 7, pp. 597–606, 2013.

[31] S.-K. Chung, "A phase tracking system for three phase utility interface inverters," *Power Electronics, IEEE Transactions on*, vol. 15, no. 3, pp. 431–438, 2000.

[32] D. Dong, B. Wen, D. Boroyevich, P. Mattavelli, and Y. Xue, "Analysis of phase-locked loop low-frequency stability in three-phase grid-connected power converters considering impedance interactions," *Industrial Electronics, IEEE Transactions on*, vol. 62, no. 1, pp. 310–321, 2015.

[33] S. Bifaretti, A. Lidozzi, L. Solero, and F. Crescimbini, "Anti-islanding detector based on a robust pll," *Industry Applications, IEEE Transactions on*, vol. 51, no. 1, pp. 398–405, 2015.

[34] J. Hu and B. Wu, "New integration algorithms for estimating motor flux over a wide speed range," *Power Electronics, IEEE Transactions on*, vol. 13, no. 5, pp. 969–977, 1998.

[35] D. Stojic, M. Milinkovic, S. Veinovic, and I. Klasnic, "Improved stator flux estimator for speed sensorless induction motor drives," *Power Electronics, IEEE Transactions on*, vol. 30, no. 4, pp. 2363–2371, 2015.

[36] N. R. N. Idris and A. H. M. Yatim, "An improved stator flux estimation in steady-state operation for direct torque control of induction machines," *IEEE Transactions on Industry Applications*, vol. 38, no. 1, pp. 110–116, 2002.

[37] M. Hinkkanen and J. Luomi, "Modified integrator for voltage model flux estimation of induction motors," *IEEE Transactions on Industrial Electronics*, vol. 50, no. 4, pp. 818–820, 2003.

[38] M.-H. Shin, D.-S. Hyun, S.-B. Cho, and S.-Y. Choe, "An improved stator flux estimation for speed sensorless stator flux orientation control of induction motors," *IEEE Transactions on Power Electronics*, vol. 15, no. 2, pp. 312–318, 2000.

[39] J. Holtz and J. Quan, "Drift-and parameter-compensated flux estimator for persistent zero-stator-frequency operation of sensorless-controlled induction motors," *Industry Applications, IEEE Transactions on*, vol. 39, no. 4, pp. 1052–1060, 2003.

[40] M. Cirrincione, M. Pucci, G. Cirrincione, and G.-A. Capolino, "A new adaptive integration methodology for estimating flux in induction machine drives," *Power Electronics, IEEE Transactions on*, vol. 19, no. 1, pp. 25–34, 2004.

Martina Kutija was born in Zadar, Croatia, in 1985. She received the Dipl.-Ing. and Ph.D. degree in electrical engineering from the University of Zagreb, Zagreb, Croatia, in 2009 and 2015, respectively. She is a Postdoctoral Research Assistant with the Department of Electrical Machines, Drives and Automation, Faculty of Electrical Engineering and Computing, University of Zagreb. Her current research interests include control of electrical drives, industrial automation and wind energy conversion systems.

Damir Sumina was born in Zagreb, Croatia, in 1978. He received the Dipl.-Ing. degree in electrical engineering from the University of Zagreb, Zagreb, Croatia, in 2001. He received the M.Sc. and Ph. D. degree in electrical engineering from the University of Zagreb, Zagreb, Croatia, in 2005 and 2009, respectively.
He is an Assistant Professor with the Department of Electrical Machines, Drives and Automation, Faculty of Electrical Engineering and Computing, University of Zagreb. His current research interests include power converters, control of electrical drives, control of synchronous generators, excitation systems, industrial automation and wind energy conversion systems.

Igor Čolović was born in Zagreb, Croatia, in 1974. He received the Dipl.-Ing. degree in electrical engineering from the University of Zagreb, Zagreb, Croatia, in 1999.
From 2000 to 2005 he was variable speed drives and industrial automation specialist with the Systec Automation, Labin, Croatia. Since 2005, he has been with Končar - Electronic and Informatics Inc., Zagreb, Croatia, where he is currently responsible for research and design of control algorithms for wind turbine converters. His current research interests include control of power converters for wind turbines and electrical drives.

AUTHORS' ADDRESSES
Martina Kutija, Ph.D.
Asst. Prof. Damir Sumina, Ph.D.
University of Zagreb,
Faculty of Electrical Engineering and Computing
Unska 3, 10000, Zagreb, Croatia
email: martina.kutija@fer.hr, damir.sumina@fer.hr
Igor Čolović
Končar - Electronics and Informatics Inc.
Fallerovo šetalište 22, 10000, Zagreb, Croatia
email: icolovic@koncar-inem.hr

Received: 2016-09-15
Accepted: 2016-10-14